

Upper bound of the charge diffusion constant in holography

Kyoung-Bum Huh,^a Hyun-Sik Jeong,^{b,c} Keun-Young Kim,^a and Ya-Wen Sun^{b,c}

^a*School of Physics and Chemistry, Gwangju Institute of Science and Technology,
123 Cheomdan-gwagiro, Gwangju 61005, Korea*

^b*School of physics & CAS Center for Excellence in Topological Quantum Computation, University
of Chinese Academy of Sciences, Zhongguancun east road 80, Beijing 100049, China*

^c*Kavli Institute for Theoretical Sciences, University of Chinese Academy of Sciences,
Zhongguancun east road 80, Beijing 100049, China*

E-mail: hkabell1689@gm.gist.ac.kr, hyunsik@ucas.ac.cn,
fortoe@gist.ac.kr, yawen.sun@ucas.ac.cn

ABSTRACT: We investigate the upper bound of charge diffusion constant in holography. For this purpose, we apply the conjectured upper bound proposal related to the equilibration scales $(\omega_{\text{eq}}, k_{\text{eq}})$ to the Einstein-Maxwell-Axion model. $(\omega_{\text{eq}}, k_{\text{eq}})$ is defined as the collision point between the diffusive hydrodynamic mode and the first non-hydrodynamic mode, giving rise to the upper bound of the diffusion constant D at low temperature T as $D = \omega_{\text{eq}}/k_{\text{eq}}^2$. We show that the upper bound proposal also works for the charge diffusion and $(\omega_{\text{eq}}, k_{\text{eq}})$, at low T , is determined by D and the scaling dimension $\Delta(0)$ of an infra-red operator as $(\omega_{\text{eq}}, k_{\text{eq}}^2) = (2\pi T \Delta(0), \omega_{\text{eq}}/D)$, as for other diffusion constants. However, for the charge diffusion, we find that the collision occurs at real k_{eq} , while it is complex for other diffusions. In order to examine the universality of the conjectured upper bound, we also introduce a higher derivative coupling to the Einstein-Maxwell-Axion model. This coupling is particularly interesting since it leads to the violation of the *lower* bound of the charge diffusion constant so the correction may also have effects on the *upper* bound of the charge diffusion. We find that the higher derivative coupling does not affect the upper bound so that the conjectured upper bound would not be easily violated.

Contents

1	Introduction	1
2	Holographic setup	4
2.1	Model	4
2.2	Fluctuations for quasi-normal modes	5
3	The upper bound: Einstein-Maxwell-Axion model	6
3.1	The equilibration scale	6
3.2	The upper bound	7
4	The upper bound with higher derivative coupling	10
4.1	Model and the lower bound: a quick review	11
4.2	The upper bound with the coupling	12
5	Conclusion	14
A	Non-hydrodynamic poles: Infra-red modes	15
B	Quasi-normal modes beyond low temperature	17

1 Introduction

Holographic methods (gauge/gravity duality) [1–4] have been providing new and effective ways to investigate the universal features in the transport properties of the strongly correlated systems. For example, in strongly coupled systems like strange metals, the resistivity (ρ) is universally linear in temperature (T), $\rho \sim T$, which is in contrary to $\rho \sim T^2$ from the Fermi liquid theory. The linear- T -resistivity ($\rho \sim T$) has been explored in holography. See [1] and references therein for the achievements with methodologies. Another example is Homes’ law. Strange metals would undergo a phase transition to the high temperature superconductor with a universal relation between the superfluid density (ρ_s), the critical temperature (T_c), and the DC electric conductivity (σ_{DC}), i.e. the so called Homes’ law: $C := \rho_s(T = 0)/(\sigma_{DC}(T_c)T_c)$, where C is universal and independent of the components of superconducting materials. For holographic studies of Homes’ law, see [5–8].

In this paper, we focus on another universal property of strongly coupled systems in holography: the identification of a universal bound of the diffusion constant (D).

One of the famous examples of the holographic bound might be the Kovtun-Son-Starinets (KSS) bound [9]¹

$$D_{\text{shear}} \geq \frac{c^2}{4\pi} \tau_{\text{pl}}, \quad (1.1)$$

where D_{shear} is the shear diffusion constant of the shear mode, c the speed of light, and $\tau_{\text{pl}} := \hbar/k_B T$ the Planckian time scale [10, 11]. The KSS bound (1.1) first appeared to be confirmed by experimental data [12–16], however it soon turns out that it can be easily violated by breaking a translational invariance [17–20].²

Lower bound of D with quantum chaos: Inspired from the violation of the KSS bound, it has been motivated to find the bound of the diffusion constant (D) in terms of the velocity (v) and the time (τ) scales:

$$D \geq v^2 \tau, \quad (1.2)$$

which is universal, for instance, not violated by breaking a translational invariance.

When the translational symmetry is broken, one may study the diffusive process governed by several diffusion constants: i) energy (or crystal) diffusion constant;³ ii) charge diffusion constant. Thus, it would be interesting to study which velocity and time scale can make a universal bound of such diffusion constants in the presence of broken translational symmetry.

It was proposed [29, 30] that the relevant scales (v, τ) for a lower bound would be related to the properties from quantum chaos as

$$v = v_B, \quad \tau = \tau_L, \quad (1.3)$$

where v_B is the butterfly velocity and τ_L the Lyapunov time. For the energy (or crystal) diffusive process, it was shown that the lower bound with quantum chaos (1.3) is robust and hard to break in many models [31–44]. Moreover, in recent years, the lower bound with (1.3) has also been understood with interesting phenomena from the ill-defined Green’s function, called pole-skipping [46, 47].

On the other hand, in the case of the charge diffusion constant, it turned out that the bound with (1.3) does not hold and could easily be violated. For instance, one of the simplest ways to break the bound of the charge diffusion constant is by considering higher derivative couplings [48].⁴

¹One can find another form of the KSS bound with $D_{\text{shear}} = \eta/(sT)$, where η is a shear viscosity, and s the entropy density.

²The KSS bound has been further investigated in numerous ways including a broken rotational symmetry or the effects of anisotropy [20–24], a higher derivative gravity [25, 26]. Moreover, recently, the relation between the momentum diffusivity and η/s has been further elaborated in [27].

³Depending on symmetry breaking patterns, one may study the energy diffusion constant (explicit symmetry breaking) or the crystal diffusion constant (spontaneous symmetry breaking). For the comprehensive review for this with the holographic toy model, see [28] and references therein.

⁴One can also see the violation of the lower bound for the charge diffusion in striped holographic matter [49], the SYK model [50]. In particular, the bound with (1.3) does not hold for the Gubser-Rocha

Diffusion	Lower bound proposal (1.3)	Upper bound proposal (1.5)
Energy (or Crystal) diffusion	Obeded	Obeded
Charge diffusion	Violated	?

Table 1. Summary of holographic studies for the bounds of diffusion constants. In this paper, we study the upper bound proposal (1.5) with the charge diffusion constant.

Upper bound of D with the hydrodynamic convergence. In the similar perspective of the lower bound, in recent years, the holographic study of the upper bound has also been investigated as

$$D \leq v^2 \tau, \quad (1.4)$$

with the simple question: the diffusion constant will also be bounded from the above? Using the idea from the convergence of hydrodynamics, it is proposed [51] that the diffusion constant may have the upper bound with the following scale⁵:

$$v = v_{\text{eq}}, \quad \tau = \tau_{\text{eq}}, \quad (1.5)$$

where $v_{\text{eq}} := \omega_{\text{eq}}/k_{\text{eq}}$ is the equilibration velocity, $\tau_{\text{eq}} := \omega_{\text{eq}}^{-1}$ the equilibration time. In order to study the upper bound with $(v_{\text{eq}}, \tau_{\text{eq}})$ in (1.5), we need to identify the equilibration scale $(\omega_{\text{eq}}, k_{\text{eq}})$. The equilibration scale is defined as the collision point in the (ω, k) space between the diffusive hydrodynamic mode (2.7) and the first non-hydrodynamic mode.

Note that the collision implies that, at such a scale, the dynamics of the system cannot be determined just by the hydrodynamic mode, i.e., the equilibration scale might be related to the radius of the convergence of hydrodynamic perturbative series [54–64]. Note also that (1.4) with (1.5) can be rewritten in terms of the equilibration scale $(\omega_{\text{eq}}, k_{\text{eq}})$ as

$$D \leq \frac{\omega_{\text{eq}}}{k_{\text{eq}}^2}, \quad (1.6)$$

where the upper bound (the equality) reflects the fact that the hydrodynamic dispersion at the quadratic order (2.7) becomes a good approximation at $(\omega_{\text{eq}}, k_{\text{eq}})$.

In this paper, our goal is to study the upper bound of the charge diffusion constant. For the energy (or crystal) diffusive process, the upper bound proposal with (1.5) has been checked in [51, 65, 66].⁶ However, the analysis for the upper bound proposal with the charge diffusion is still missing, thus we fill this gap in this paper. See table 1 for the summary of the studies of the (lower/upper) bounds in holography. Moreover, we also investigate the upper bound of the charge diffusion constant in the presence of the higher derivative

model [44], giving a divergence in the low T limit ($m/T \gg 1$). See also the case with massive gravity models [45].

⁵More generally, it has been argued that the local equilibration time may set an upper bound on the diffusivity in [52, 53].

⁶In [51], authors also checked that the upper bound proposal works for the shear diffusion constant in the translational invariant system.

coupling [48] to examine the universality of the conjectured upper bound proposal (1.5).

This paper is organized as follows. In section 2, we introduce the gravity model to study the charge diffusion in holography. In section 3, we study the upper bound of the charge diffusion constant with the model presented in section 2. In section 4 we investigate the effect of the higher derivative coupling for the upper bound of the charge diffusion constant. Section 5 is devoted to conclusions.

2 Holographic setup

2.1 Model

We consider the Einstein-Maxwell-Axion model [67] in (3+1) dimensions

$$S = \int d^4x \sqrt{-g} \left[R + \frac{6}{L^2} - \frac{1}{4} F^2 - \frac{1}{2} \sum_{i=1}^2 (\partial \varphi_i)^2 \right], \quad (2.1)$$

where we set the gravitational constant $16\pi G = 1$ and we have included two matter fields: a U(1) gauge field A with the field strength $F = dA$ and the massless scalar fields $\varphi_i = mx^i$ where m denotes the strength of the translational symmetry breaking.

The model (2.1) allows the analytic background solution as

$$\begin{aligned} ds^2 &= -f(r)dt^2 + \frac{dr^2}{f(r)} + \frac{r^2}{L^2}(dx^2 + dy^2), \\ f(r) &= \frac{r^2}{L^2} \left(1 + \frac{L^2 \mu^2 r_h^2}{4r^4} - \frac{L^4 m^2}{2r^2} - \frac{r_h^3}{r^3} \left(1 + \frac{L^2 \mu^2}{4r_h^2} - \frac{L^4 m^2}{2r_h^2} \right) \right), \\ A &= \mu \left(1 - \frac{r_h}{r} \right) dt, \quad \varphi_i = mx^i, \end{aligned} \quad (2.2)$$

where $f(r)$ is the emblackening factor, r_h is the black hole horizon, and μ denotes the chemical potential of the boundary field theory, $\mu = \lim_{r \rightarrow \infty} A_t$. From here we set $L = 1$.

The thermodynamic quantities from (2.2) read

$$T = \frac{f'(r_h)}{4\pi} = \frac{1}{4\pi} \left(3r_h - \frac{\mu^2 + 2m^2}{4r_h} \right), \quad \rho = \mu r_h, \quad (2.3)$$

where ρ is interpreted as the expectation value of charge density.

Charge diffusion constant in holography: Here we introduce the charge diffusion constant (D_c) as

$$D_c := \frac{\sigma}{\chi}, \quad \sigma = 1 + \frac{\mu^2}{m^2}, \quad \chi = \left(\frac{\partial \rho}{\partial \mu} \right)_T, \quad (2.4)$$

where σ is the electric conductivity [67] and χ is the compressibility. One can see that m makes the conductivity finite as the reflection of the broken translational invariance.

At finite charge density, the generalized Einstein relation [68] shows the charge diffusion constant is coupled with the energy diffusion constant, i.e., in order to focus on the charge

diffusion constant, we need to consider the zero charge density (or zero chemical potential) case. Therefore, we set $\mu = 0$ in this paper.⁷ The charge diffusion constant (2.4) at zero charge can be expressed as

$$D_c = \frac{6}{4\pi T + \sqrt{6m^2 + 16\pi^2 T^2}}. \quad (2.5)$$

Note that the upper bound of the energy diffusion constant at $\mu = 0$ has been investigated in [51].

2.2 Fluctuations for quasi-normal modes

Based on the background solution (2.2) at zero charge, we consider the following gauge field fluctuations

$$\delta A_t(r, t, x, y) = \delta \bar{A}_t(r) e^{-i\omega t + ikx}, \quad \delta A_x(r, t, x, y) = \delta \bar{A}_x(r) e^{-i\omega t + ikx}, \quad (2.6)$$

which is relevant to the study of the hydrodynamic charge diffusion mode [69]:

$$\omega = -i D_c k^2, \quad (2.7)$$

where D_c corresponds to (2.5).

After Fourier transformation, one can find one single fluctuation equation of motion

$$0 = Z_A''(r) + \frac{r^3 \omega^2 f'(r) - 2k^2 f(r)^2}{r f(r) (r^2 \omega^2 - k^2 f(r))} Z_A'(r) + \frac{r^2 \omega^2 - k^2 f(r)}{r^2 f(r)^2} Z_A(r), \quad (2.8)$$

by introducing the variable

$$Z_A(r) := k \delta \bar{A}_t(r) + \omega \delta \bar{A}_x(r), \quad (2.9)$$

where it is composed of field fluctuations in (2.6).

In order to study the quasi-normal mode spectrum for both the charge diffusion mode (the lowest mode) and the higher modes, we need to solve the equation of motion (2.8) with two boundary conditions: one from the horizon and the other from the AdS boundary. Near the horizon, we impose the incoming boundary condition as

$$Z_A = (r - r_h)^{\nu_-} \left(Z_A^{(I)} + Z_A^{(II)}(r - r_h) + \dots \right), \quad (2.10)$$

where $\nu_- := -i\omega/4\pi T$ and $Z_A^{(I,II)}$ are horizon coefficients. Near the AdS boundary, the solution is expanded as

$$Z_A = Z_A^{(S)}(1 + \dots) + Z_A^{(R)} r^{-1}(1 + \dots), \quad (2.11)$$

⁷At finite charge, the charge diffusion constant might be decoupled from the energy diffusion constant in the strong momentum relation limit [44]. In this paper, we only focus on the simplest case to study the charge diffusion constant: the $\mu = 0$ case. We leave the study of the upper bound at finite charge in the strong momentum relaxation regime as future work.

where $Z_A^{(S)}$ is interpreted as the source term and $Z_A^{(R)}$ is for the response term via AdS/CFT dictionary. Then, the quasi-normal mode spectrum can be found by the values of (ω, k) where the source term $Z_A^{(S)}$ in (2.11) is zero.

3 The upper bound: Einstein-Maxwell-Axion model

In this section, we evaluate the quasi-normal modes from (2.8) and study the upper bound of the charge diffusion constant, (1.6), with the equilibration scale $(\omega_{\text{eq}}, k_{\text{eq}})$. In particular, we mainly focus on the low temperature (T) case because the upper bound is approached at low T . For the discussion beyond low T , see appendix B.

3.1 The equilibration scale

The equilibration scale $(\omega_{\text{eq}}, k_{\text{eq}})$ is defined as the collision point in (ω, k) space between the hydrodynamic mode (2.7) and the first non-hydrodynamic mode, i.e., the equilibration scale is related to the breakdown of the hydrodynamics.

Non-hydrodynamic modes (IR modes): Let us first explain the non-hydrodynamic modes. At low T , it is shown that the non-hydrodynamic modes correspond to the IR modes from IR green's function \mathcal{G}_{IR} [51, 66]. We present \mathcal{G}_{IR} of the fluctuation for the charge diffusion (2.9) as

$$\mathcal{G}_{\text{IR}} = \left(\frac{3}{\pi}\right)^{1-2\Delta(0)} T^{1-2\Delta(0)} \frac{\Gamma\left(\frac{1}{2} - \Delta(0)\right) \Gamma\left(\Delta(0) - \frac{i\omega}{2\pi T}\right)}{\Gamma\left(\Delta(0) - \frac{1}{2}\right) \Gamma\left(1 - \Delta(0) - \frac{i\omega}{2\pi T}\right)}, \quad (3.1)$$

where $\Delta(0)$ is the scaling dimension of operator at the IR fixed point at zero wavevector.⁸ Then, one can find the IR modes from the IR green's function (3.1) as

$$\omega_n = -i 2\pi T(n + \Delta(0)), \quad n = 0, 1, 2, \dots, \quad (3.2)$$

where $\Delta(0) = 1$ from (A.7).

The equilibration scale $(\omega_{\text{eq}}, k_{\text{eq}})$: In Fig. 1, we display the representative result of quasi-normal modes at low T . From the figure, one can see that quasi-normal modes are well approximated with i) the hydrodynamic mode (solid line) (2.7); ii) the IR modes (dashed line) (3.2). In particular, from the gray region in Fig. 1, the equilibration scale $(\omega_{\text{eq}}, k_{\text{eq}})$ can be obtained from the collision (ω_c, k_c) between the hydrodynamic mode and the first non-hydrodynamic mode.

The equilibration scale $(\omega_{\text{eq}}, k_{\text{eq}})$ is defined as the collision point (ω_c, k_c) in absolute value

$$\omega_{\text{eq}} := |\omega_c|, \quad k_{\text{eq}} := |k_c|, \quad (3.3)$$

⁸We also present all the details for (3.1) in appendix A in a self-contained manner.

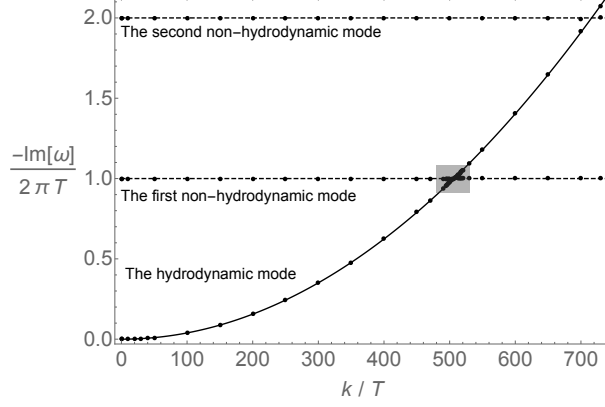


Figure 1. Quasi-normal modes at $m/T = 10^5$. All dots represent quasi-normal modes. The solid line is the hydrodynamic mode (2.7), and the dashed lines are IR modes (3.2). In the gray square region, one can see the collision between the hydrodynamic mode and the first non-hydrodynamic mode.

because the collision occurred in the complex (ω, k) space for the cases with other diffusion constants [51, 65, 66], satisfying

$$\omega_c = \omega_{\text{eq}} e^{i(\phi_k - \frac{\pi}{2})}, \quad k_c = k_{\text{eq}} e^{i\phi_k}, \quad (3.4)$$

where the finite phase ϕ_k , $\phi_k \neq 0$, produces a complex (ω_c, k_c) .

However, for the charge diffusion case, we found that the collision occurs in the real wavevector k , i.e.,

$$\phi_k = 0, \quad (3.5)$$

which is a distinct feature not observed in other diffusion cases [51, 65, 66]. In Fig. 2, we present how the hydrodynamic mode collides with the first non-hydrodynamic mode at real k . In Fig. 2(a), the collision point (ω_c, k_c) is denoted as the red star. Note that, after the collision (red star), the quasi-normal modes would be a complex value with real ω and become pure imaginary at larger k . See Fig. 2(b).

The temperature dependence in $(\omega_{\text{eq}}, k_{\text{eq}})$: In Fig. 3, we show that the equilibration scale has the following temperature dependence as

$$\frac{\omega_{\text{eq}}}{2\pi T} \sim \Delta(0) + \# \sqrt{T}, \quad \frac{k_{\text{eq}}}{T} \sim \frac{\#}{\sqrt{T}}, \quad (3.6)$$

where $\Delta(0) = 1$ from (A.7). Note that the red circle in Fig. 3 corresponds to the collision point (red star) in Fig. 2.

3.2 The upper bound

The upper bound of the charge diffusion constant (D_c): With the conjectured upper bound proposal in (1.6), now we study the upper bound of the charge diffusion

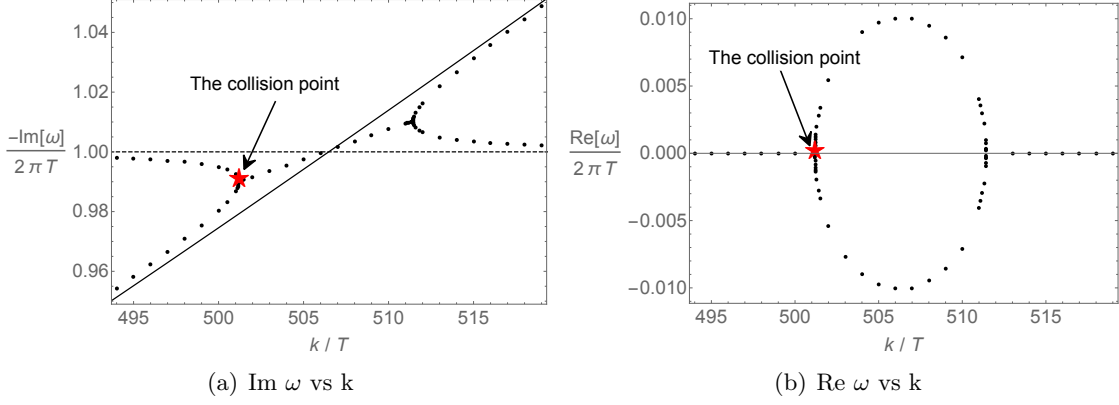


Figure 2. The collision between the hydrodynamic mode and the first non-hydrodynamic mode. The left figure is the zoom of the gray region in Fig. 1. The red star corresponds to the collision point (ω_c, k_c) .

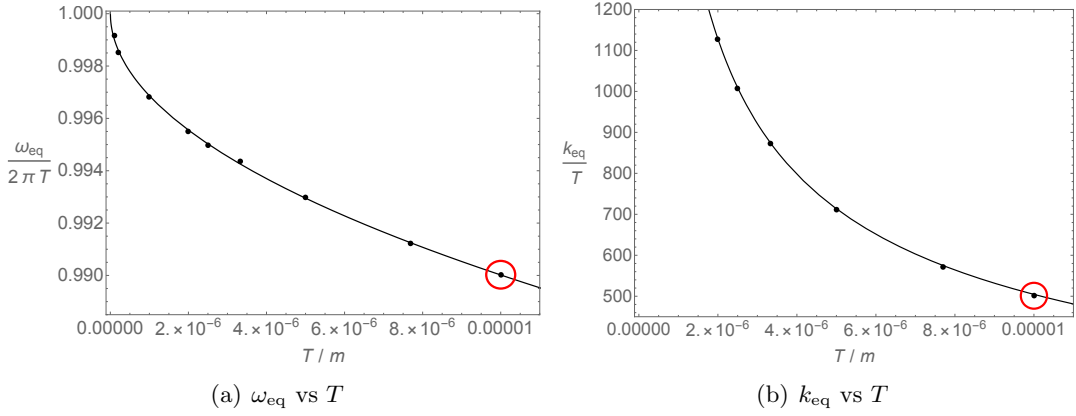


Figure 3. The temperature dependence of ω_{eq} and k_{eq} . Dots are numerical data and the solid lines are fitting curves (3.6). The red circle corresponds to the collision point (red star) in Fig. 2.

constant (D_c):

$$D_c \leq \frac{\omega_{\text{eq}}}{k_{\text{eq}}^2}, \quad (3.7)$$

where D_c is (2.5) and the equilibration scale $(\omega_{\text{eq}}, k_{\text{eq}})$ is (3.6).

In Fig. 4, we show that the conjectured upper bound proposal is valid for the case of the charge diffusion. In other words, the equality in (3.7) is approached at low T . Note that the upper bound (or the equality) implies that, at low T , the quadratic hydrodynamic mode (2.7) becomes a good approximation even at $(\omega_{\text{eq}}, k_{\text{eq}})$, i.e.,

$$1 = \frac{k_{\text{eq}}^2 D_c}{\omega_{\text{eq}}} \rightarrow \omega_{\text{eq}} = D_c k_{\text{eq}}^2, \quad (3.8)$$

which also can be checked in Fig. 5.

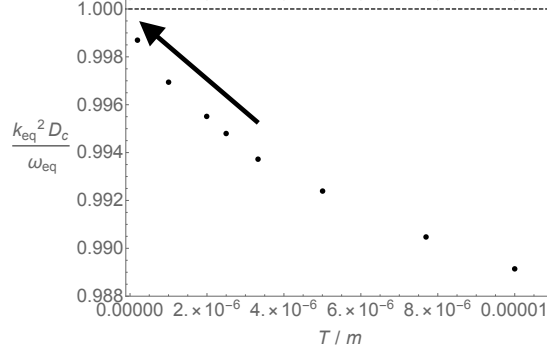


Figure 4. The upper bound of the charge diffusion constant. The dashed line denotes the upper bound (or the equality) in (3.7).

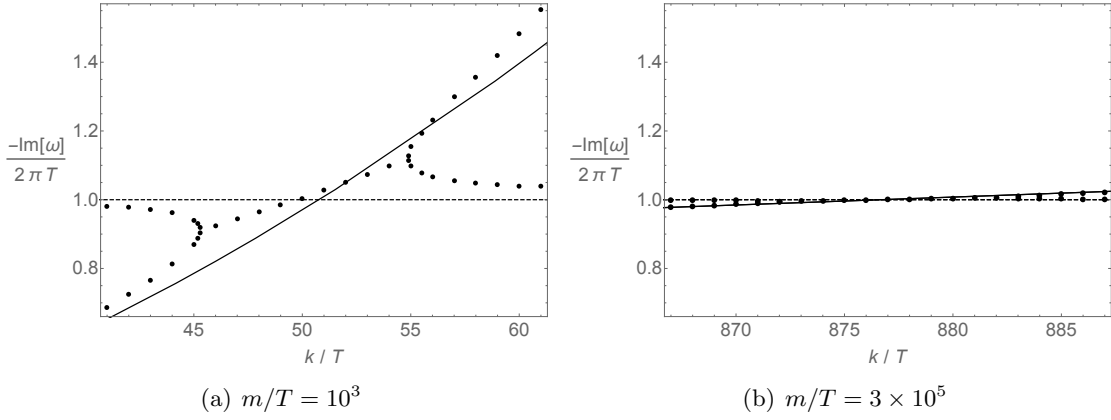


Figure 5. Quasi-normal modes with different T . As the temperature T is lowered from Fig. 5(a) to Fig. 5(b), quasi-normal modes (dots) are getting better and better approximated with hydrodynamic mode (solid line) (2.7) and IR modes (dashed line) (3.2).

Further comments on the upper bound of the diffusion constants (D): In the previous paragraph, we show that the upper bound proposal (1.6) is also valid for the charge diffusion constant in addition to other diffusion constants [51, 65, 66]. This may imply that there would be a universal feature for the upper bound proposal, which can be appeared with any diffusion constant D at low T . Thus, we may investigate further (1.6) with the low T analysis to find such a universality.

First, let us consider the following low T behavior of $(\omega_{\text{eq}}, k_{\text{eq}})$ with D as

$$\begin{aligned} \omega_{\text{eq}} &= \left(\Delta(0) + c_1 \left(\frac{T}{\Gamma} \right)^{p_1} \right) 2\pi T, & k_{\text{eq}} &= \frac{c_2}{\left(\frac{T}{\Gamma} \right)^{p_2}} T, \\ D &= \frac{c_3}{\Gamma} + c_4 \left(\frac{T^{p_3-1}}{\Gamma^{p_3}} \right), \end{aligned} \quad (3.9)$$

where c_i are coefficients, p_i the T -scaling power, and Γ is an additional factor for the

dimensionless analysis.⁹ For instance, in the case of $\Gamma = m$, the scaling power (p_i) would be

$$\begin{aligned} \text{Energy diffusion: } p_1 &= 1, & p_2 &= \frac{1}{2}, & p_3 &= 3, \\ \text{Charge diffusion: } p_1 &= \frac{1}{2}, & p_2 &= \frac{1}{2}, & p_3 &= 2, \end{aligned} \quad (3.10)$$

where the energy diffusion is from [51] and the charge diffusion case can be read from (3.6) with (2.5).

With (3.9), the upper bound of the diffusion constant, the equality in (1.6), can be expanded at low T as

$$\frac{k_{\text{eq}}^2 D}{\omega_{\text{eq}}} = \frac{(c_2)^2 c_3}{2\pi\Delta(0)} \left(\frac{T}{\Gamma}\right)^{1-2p_2} + \dots, \quad (3.11)$$

where \dots denotes sub-leading terms in T . From this leading order result (3.11), we may notice two things. First, in order to have a universal upper bound independent of T , p_2 should be universal as

$$\text{any diffusion constant } D: \quad p_2 = \frac{1}{2}, \quad (3.12)$$

for all D , which can also be observed in (3.10) as well as in other cases [51, 65, 66]. Second, there would be a non-trivial relation between coefficients c_i and $\Delta(0)$ to have the same upper bound, i.e.,

$$\frac{k_{\text{eq}}^2 D}{\omega_{\text{eq}}} = \frac{(c_2)^2 c_3}{2\pi\Delta(0)} = 1, \quad (3.13)$$

where the last equality is verified by the case of the charge diffusion as well as other diffusion cases [51, 65, 66].¹⁰ Note that, even for the case of the same diffusion constant D , $\Delta(0)$ would be different depending on Γ so that one may not easily expect the relation in the last equality in (3.13): for instance, for the energy diffusion, $\Delta(0) = 2$ for $\Gamma = m$ (m is an axion charge) [51], while $\Delta(0) = 1$ for $\Gamma = H$ (H is a magnetic field) [66].

4 The upper bound with higher derivative coupling

In the previous section, we show that the conjectured upper bound also works for the charge diffusion constant, i.e., our work would be complementary to previous studies of upper bound of other diffusion constants [51, 65, 66].

As demonstrated in the introduction, it was shown that the charge diffusion may not have a universal “lower” bound in holography. One of the representative examples is a simple gravity model with a higher derivative coupling [48].

⁹Note that dimensionless quantities would be $(\omega_{\text{eq}}/T, k_{\text{eq}}/T, DT)$ together with Γ/T .

¹⁰ c_3 in (3.9) might be understood analytically, however c_2 mostly would be obtained from numerics by fitting so that the last equality in (3.13) would be non-trivial.

In this section, we further investigate the “upper” bound of the charge diffusion constant in the presence of the higher derivative coupling to examine the universality of the conjectured upper bound proposal.

First, we review the higher derivative model and how the higher derivative coupling breaks the lower bound of the charge diffusion constant. Then we discuss the upper bound with the coupling.

4.1 Model and the lower bound: a quick review

Gauge-axion coupling model: Let us consider the higher derivative coupling model [48]

$$S = \int d^4x \sqrt{-g} \left[R + 6 - \frac{1}{4} F^2 - \text{Tr}[\mathcal{X}] - \frac{J}{4} \text{Tr}[\mathcal{X} F^2] \right], \quad (4.1)$$

where

$$\mathcal{X}^\mu{}_\nu \equiv \frac{1}{2} \sum_{i=1}^2 \partial^\mu \varphi^i \partial_\nu \varphi^i, \quad \text{Tr}[\mathcal{X} F^2] \equiv [\mathcal{X}]^\mu{}_\nu F^\nu{}_{\nu'} F^{\nu'}{}_\mu. \quad (4.2)$$

Note that (4.1) becomes the Einstein-Maxwell-Axion model (2.1) at zero coupling, $J = 0$.¹¹

The coupling J does not affect the background equations of motion [48] so that (4.1) allows the same analytic solution (2.2) with the temperature (2.3).

D_c with the butterfly velocity v_B (the lower bound): The lower bound of the charge diffusion constant in (4.1) can be studied with the following electric conductivity (σ), the butterfly velocity (v_B), and the Lyapunov time (τ_L)

$$\sigma = 1 - J \frac{m^2}{4r_h^2}, \quad v_B^2 = \frac{\pi T}{r_h}, \quad \tau_L = \frac{1}{2\pi T}, \quad (4.3)$$

at $\mu = 0$.¹² Recall that we need to consider the case at zero charge density for the study of the charge diffusion decoupled from the energy diffusion.

Using (4.3) with the definition of D_c in (2.4), one can find that the charge diffusion constant and the butterfly velocity behave at low T as

$$\frac{D_c}{\tau_L} \sim \frac{\sqrt{6}\pi(2-3J)}{m/T}, \quad \frac{1}{v_B^2} \sim \frac{1}{\sqrt{6}\pi} \frac{m}{T}, \quad (4.4)$$

where the horizon r_h is replaced by T (2.3). Then, we have the lower bound of the charge diffusion constant, (1.3), from (4.4) as

$$\mathcal{B}_L := \frac{D_c}{v_B^2 \tau_L} = 2 - 3J, \quad (4.5)$$

where it is approached at low T . For instance, see the case of $J = 1/3$ in Fig. 6. From

¹¹The causality and the stability condition give the constraint to J as $0 \leq J \leq 2/3$ [48].

¹²For the details of (4.3), see [48].

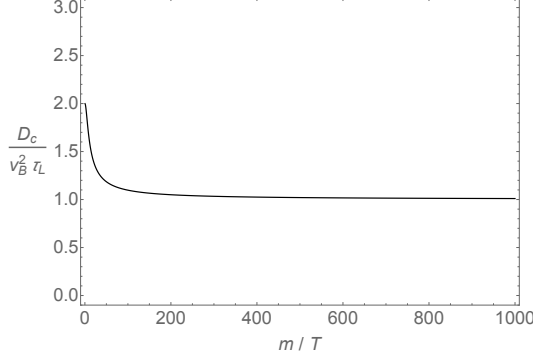


Figure 6. The lower bound of D_c at $J = 1/3$, which approaches $\mathcal{B}_L = 1$ in (4.5) at low T ($m/T \gg 1$).

(4.5), we can see that the coupling J can break the lower bound of the charge diffusion constant, i.e., $\mathcal{B}_L = 0$ at $J = 2/3$.

4.2 The upper bound with the coupling

Next, we study the upper bound of the charge diffusion, (1.5), at a finite coupling J . For this purpose, we need to investigate the coupling dependence in $(\tau_{\text{eq}}, v_{\text{eq}})$.

The equilibration time scale τ_{eq} : Following the same procedure in appendix A, τ_{eq} can be read from the IR modes. We found that the fluctuation equation of motion of (4.1) is

$$0 = \partial_\zeta^2 Z_A + \left(\frac{2\zeta}{\zeta^2 - \zeta_h^2} - \frac{(36 - 54J)\zeta k^2}{9(2 - 3J)k^2(\zeta^2 - \zeta_h^2) - \zeta_\omega^2 m^2} \right) \partial_\zeta Z_A + \left(\frac{\zeta_\omega^2}{9(\zeta^2 - \zeta_h^2)^2} - \frac{(2 - 3J)k^2}{m^2(\zeta^2 - \zeta_h^2)} \right) Z_A, \quad (4.6)$$

where the extremal geometry is (A.3)¹³ and also note that (4.6) becomes (A.5) at $J = 0$.

From (4.6), one can see that the coupling is always coupled to the wavevector k . This means that τ_{eq} is independent of the coupling because ω_{eq} is evaluated at $k = 0$ (A.10), i.e.,

$$\tau_{\text{eq}} := 1/\omega_{\text{eq}} = \frac{1}{2\pi T \Delta(0)} = \tau_L, \quad (4.7)$$

where (4.3) is used in the last equality with $\Delta(0) = 1$ (A.7).

The equilibration velocity scale v_{eq} : The velocity scale can be obtained as follows.

$$v_{\text{eq}}^2 := \frac{\omega_{\text{eq}}^2}{k_{\text{eq}}^2} = \omega_{\text{eq}} D_c, \quad (4.8)$$

¹³Recall that the background geometry is not affected by the coupling J .

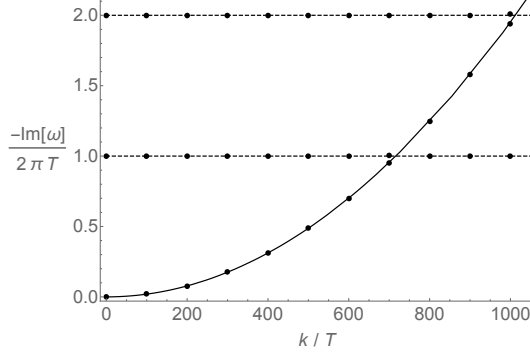


Figure 7. Quasi-normal modes at $J = 1/3$ with $m/T = 10^5$. The solid line is the hydrodynamic mode (2.7). The dashed lines are IR modes (3.2).

where we used (3.8) in the second equality. Note that it would be nontrivial if (3.8) is also valid at finite J : recall that (3.8) implies that, at low T , the quasi-normal modes are well approximated by both the hydrodynamic mode (2.7) and the IR modes (3.2). We have numerically checked that (3.8) would also be valid at finite J .¹⁴ For instance, see the representative example for $J = 1/3$ in Fig. 7.¹⁵

With the time scale (4.7), the equilibration velocity (4.8) can be further expressed as

$$v_{\text{eq}}^2 = \omega_{\text{eq}} D_c = \frac{D_c}{\tau_L}, \quad (4.9)$$

and, using (4.4), one can find the relation between the equilibration velocity and the butterfly velocity as

$$v_{\text{eq}}^2 = (2 - 3J) v_B^2. \quad (4.10)$$

Thus, the coupling J does not affect τ_{eq} (4.7), but v_{eq} (4.10).

D_c with the equilibration velocity v_{eq} (the upper bound): Then, now one can find the upper bound of the charge diffusion at finite J as

$$\mathcal{B}_U := \frac{D_c}{v_{\text{eq}}^2 \tau_{\text{eq}}} = \frac{D_c}{v_B^2 \tau_L} \frac{1}{2 - 3J} =: \mathcal{B}_L \frac{1}{2 - 3J}, \quad (4.11)$$

where we used (4.7) and (4.10). One may think that the upper bound (\mathcal{B}_U) in (4.11) is diverging at $J = 2/3$ so that the coupling also breaks the upper bound as well as the lower bound (\mathcal{B}_L) in (4.5). However, the upper bound would be still valid at finite coupling J , because \mathcal{B}_L in (4.5) cancels out the coupling dependence, $1/(2 - 3J)$, in (4.11), in other words, we have $\mathcal{B}_U = 1$ for all J .

¹⁴As $J \rightarrow 2/3$, we checked that D_c is decreasing (4.4), while k_{eq} increases so that (3.8) would be respected at $J \rightarrow 2/3$.

¹⁵(3.8) at finite J is already implying that the upper bound proposal is valid at finite coupling.

5 Conclusion

We have studied the upper bound of the charge diffusion constant with the conjectured upper bound proposal [51, 65, 66]:

$$D \leq \frac{\omega_{\text{eq}}}{k_{\text{eq}}^2}, \quad (5.1)$$

where the equilibration scale $(\omega_{\text{eq}}, k_{\text{eq}})$ is identified with the collision point between the diffusive hydrodynamic mode and the first non-hydrodynamic mode. The upper bound (an equality) in (5.1) is approached at low T with

$$\omega_{\text{eq}} \rightarrow 2\pi T \Delta(0), \quad k_{\text{eq}}^2 \rightarrow \frac{\omega_{\text{eq}}}{D}, \quad (5.2)$$

which implies that the hydrodynamic mode at quadratic order (2.7) would be a good approximation even around the equilibration scale.

Charge diffusion constant and the upper bound: We check that the upper bound proposal (5.1) also works for the charge diffusion constant, D_c , in addition to other diffusion constants: energy diffusion constant [51, 66], shear diffusion constant [51], crystal diffusion constant [65, 66]. This implies that there would be a universal property for the upper bound, independent of the type of diffusion constants. From the low temperature (T) analysis in (3.9), we found that k_{eq} plays the major role in the upper bound of any diffusion constant D , as

$$\frac{k_{\text{eq}}^2 D}{\omega_{\text{eq}}} \sim T^{1-2p_2}, \quad (5.3)$$

where p_2 is from $k_{\text{eq}} \sim T^{1-p_2}$. Thus, one can notice that p_2 should be universal as $p_2 = 1/2$ in order to have the upper bound (or a T -independent quantity).

In addition to the universal feature, $p_2 = 1/2$, we also found that the charge diffusion case would have a distinct feature in the phase of k , ϕ_k , in (3.4), which is not observed in other diffusion constants:

$$\text{Charge diffusion : } \phi_k = 0, \quad \text{Other diffusions : } \phi_k \neq 0. \quad (5.4)$$

For instance, energy diffusion constant has a finite T -dependence as $\phi_k \sim T^{7/2-\Delta(0)}$ [66]. Note that (5.4) implies the collision occurs at a real wavevector for the charge diffusion while it is complex for other diffusions [51, 65, 66].¹⁶

It is investigated that the quantum chaos property would be related with the pole-skipping phenomena in the “upper”-half-frequency-plane [46]. However, the pole-skipping point of the charge diffusion is in the “lower”-half-frequency-plane [72, 73] so that the charge diffusion may not be related to quantum chaos. The real wavevector collision in (5.4), $\phi_k = 0$, might be a new piece of supporting evidence for this. Note that one of the

¹⁶In [70], it was shown that the radius of convergence of linear hydrodynamics in liquids is also related to the real wavevector, called k-gap [71].

signals of the quantum chaos is the level repulsion from random matrix theory [74–76], i.e., the quantum chaos property might be related to the case with $\phi_k \neq 0$ in our language.

Universal upper bound: We further investigated the upper bound of the charge diffusion constant with the higher derivative couplings and found that, unlike the lower bound (4.5), the coupling cannot break the upper bound of the charge diffusion constant (4.11), thus we speculate that the conjectured upper bound

$$\frac{k_{\text{eq}}^2 D_c}{\omega_{\text{eq}}} = 1, \quad (5.5)$$

would be universal independent of the couplings (or UV data), but only depends on the IR fixed points as in the universal lower bound of the energy diffusion constant.¹⁷ It would be interesting to investigate how (5.5) (as well as the case with other diffusion constants) can be generalized to generic IR fixed points.¹⁸ We leave this subject as future work and hope to address it in the near future.

Acknowledgments

We would like to thank Yongjun Ahn, Matteo Baggioli, Wei-Jia Li, Yan Liu, Xin-Meng Wu for valuable discussions and correspondence. We thank Yan Liu, Xin-Meng Wu for sharing with us unpublished results. This work was supported by the National Key R&D Program of China (Grant No. 2018FYA0305800), Project 12035016 supported by National Natural Science Foundation of China, the Strategic Priority Research Program of Chinese Academy of Sciences, Grant No. XDB28000000, Basic Science Research Program through the National Research Foundation of Korea (NRF) funded by the Ministry of Science, ICT & Future Planning (NRF- 2021R1A2C1006791) and GIST Research Institute (GRI) grant funded by the GIST in 2021. K.-B. Huh and H.-S. Jeong contributed equally to this paper and should be considered co-first authors.

A Non-hydrodynamic poles: Infra-red modes

It was shown that non-hydrodynamic modes are associated with infra-red Green’s function [51, 66]. The infra-red Green’s function can be calculated by solving the fluctuation equation in the extremal geometry with scaling dimension $\Delta(k)$ at the infra-red fixed point. For the details, we refer the readers to [66].

¹⁷We are grateful to Yan Liu and Xin-Meng Wu for sharing the preliminary results for the case of the charge diffusion in the conformal to AdS₂ fixed point [77]: it seems that the gauge coupling may play an important role to study the upper bound as well the IR geometry. For the detailed discussion and extension, we refer to their forthcoming work [77].

¹⁸Recall that (5.5) is for the AdS₂ fixed point. We expect that there could be a universal constant on the right hand side of (5.5) because the leading constant at low T does not depend on the UV data (T, Γ) as can be seen in (3.13).

The extremal geometry: From (2.3), we can consider the following relation at zero temperature:

$$r_h = r_e, \quad r_e = \frac{m}{\sqrt{6}}. \quad (\text{A.1})$$

Moreover, considering the following coordinate transformation, one can have the extremal geometry

$$r = r_e + \epsilon \zeta, \quad r_h = r_e + \epsilon \zeta_h, \quad t = \frac{u}{\epsilon}, \quad (\text{A.2})$$

where $\zeta_h = 4\pi\delta T/9$ represents a small temperature correction.

Considering (A.2) in the $\epsilon \rightarrow 0$ limit, the metric of (2.2) is transformed into the extremal geometry as

$$ds^2 = -\frac{\zeta^2}{L_2^2} \left(1 - \frac{\zeta_h}{\zeta}\right)^2 du^2 + \frac{L_2^2}{\zeta^2 \left(1 - \frac{\zeta_h}{\zeta}\right)^2} dr^2 + r_e^2 (dx^2 + dy^2), \quad (\text{A.3})$$

where the AdS₂ radius L_2 is $\sqrt{1/6}$.

Fluctuation equation for IR modes: Similarly, we can do the coordinate transformation in the Fourier space as

$$r = r_e + \epsilon \zeta, \quad r_h = r_e + \epsilon \zeta_h, \quad \omega = \epsilon \zeta_\omega, \quad (\text{A.4})$$

and from this transformation we can express the fluctuation equation (2.8) in the extremal geometry as

$$\begin{aligned} 0 = & \partial_\zeta^2 Z_A + \left(\frac{2\zeta}{\zeta^2 - \zeta_h^2} - \frac{36\zeta k^2}{18k^2(\zeta^2 - \zeta_h^2) - \zeta_\omega^2 m^2} \right) \partial_\zeta Z_A \\ & + \left(\frac{\zeta_\omega^2}{9(\zeta^2 - \zeta_h^2)^2} - \frac{2k^2}{m^2(\zeta^2 - \zeta_h^2)} \right) Z_A, \end{aligned} \quad (\text{A.5})$$

where the second term of the first derivative of (A.5), the k -dependent term, did not appear in other diffusion cases [51, 65, 66].

In the AdS₂ boundary ($\zeta \rightarrow \infty$), the solution for (A.5) can be expanded:

$$Z_A = Z^{(S)} \zeta^{\Delta(k)-1} + Z^{(R)} \zeta^{-\Delta(k)}, \quad (\text{A.6})$$

where $Z_A^{(S)}$ is interpreted as the source term and $Z_A^{(R)}$ is for the response term and $\Delta(k)$ is the operator of dimension at the infra-red fixed point

$$\Delta(k) = \frac{1}{2} + \frac{\sqrt{8k^2 + m^2}}{2m}. \quad (\text{A.7})$$

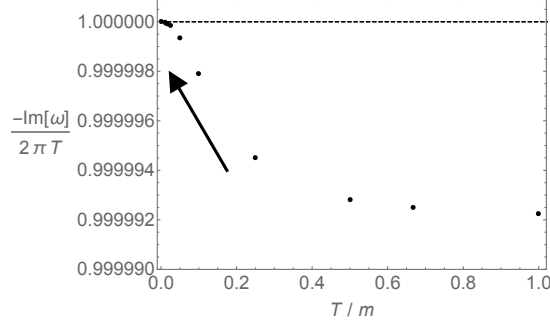


Figure 8. The first-non hydrodynamic mode at $k/T = 1/100$. Poles (black dots) are approaching the IR mode (dashed line) (A.10), the first IR mode (ω_0), at low T .

The non-hydrodynamic modes: According to the holographic dictionary, the infrared Green’s function, \mathcal{G}_{IR} , can be calculated by solving the fluctuation equation (A.5) near the AdS_2 boundary ($\zeta \rightarrow \infty$) [78, 79]:

$$\mathcal{G}_{\text{IR}} \propto \frac{Z^{(R)}}{Z^{(S)}}, \quad (\text{A.8})$$

where $Z^{(R)}$ and $Z^{(S)}$ are the coefficients of the solution (A.6), respectively.

Then one can find \mathcal{G}_{IR} at $k = 0$ ¹⁹ as

$$\mathcal{G}_{\text{IR}} = \left(\frac{3}{\pi}\right)^{1-2\Delta(0)} T^{1-2\Delta(0)} \frac{\Gamma(\frac{1}{2} - \Delta(0)) \Gamma(\Delta(0) - \frac{i\omega}{2\pi T})}{\Gamma(\Delta(0) - \frac{1}{2}) \Gamma(1 - \Delta(0) - \frac{i\omega}{2\pi T})}, \quad (\text{A.9})$$

where the pole of the \mathcal{G}_{IR} of (A.9), IR modes, are

$$\omega_n = -i 2\pi T(n + \Delta(0)), \quad n = 0, 1, 2, \dots, \quad (\text{A.10})$$

with $\Delta(0) = 1$ from (A.7). In Fig. 8, we show that the non-hydrodynamic pole is approaching the IR modes (A.10) at low T .

B Quasi-normal modes beyond low temperature

In Sec. 3, we mainly focused on the “low” temperature regime ($m/T \gg 1$) in order to study the bound of the charge diffusion constant, showing that, at low T , the quasi-normal modes are well approximated with i) the hydrodynamic mode (2.7); ii) the IR modes (A.10). See Fig. 1.

Motivation: In this section, we further investigate the quasi-normal modes at “higher” temperature (i.e., smaller m/T) to show how (2.7) and (A.10) would be good approximations to the quasi-normal modes at low T . To our knowledge, our work is the first holographic study showing the excellent applicability of approximations ((2.7), (A.10)) in

¹⁹We focus on the case at $k = 0$, which is sufficient for the non-hydrodynamic mode [51, 66].

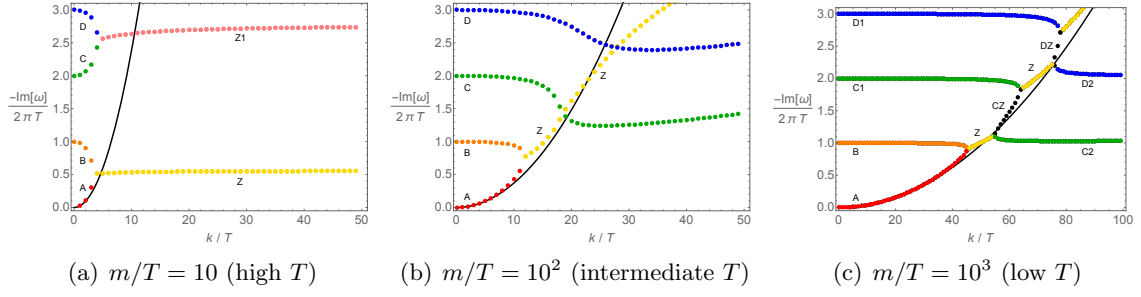


Figure 9. Quasi-normal modes from high T to low T . All dots are quasi-normal modes and the black solid line is the charge diffusion mode (2.7). Note that the region around $k/T \sim 50$ in Fig. 9(c) corresponds to Fig. 5(a).

terms of the full dynamics of quasi-normal modes from high T to low T .²⁰ Although we focused on the charge diffusion constant in this paper, we believe similar dynamics may occur in the case of other diffusion constants [51, 65, 66].²¹

Quasi-normal modes at high T : First, let us show the representative result of high T in Fig. 9(a).²² At high T , one can find that there is a feature in the quasi-normal modes: the structure consisting of three lines (e.g., A (red), B (orange), Z (yellow)) repeats in the frequency ω direction. As we decrease the temperature, the structure in Fig. 9(a) would change into what we observed in Sec. 3 (e.g., Fig. 1). Now one may notice that it is non-trivial to obtain the low T result (e.g., Fig. 1) from the high T result (e.g., Fig. 9(a)).

We find that as T decreases, Z (yellow) in Fig. 9(a) plays an important role in obtaining the low T result. In particular, the low T result can be understood by the interaction between Z and the non-hydrodynamic mode (C and D) in Fig. 9(a). We explain this further in two steps: i) $Z1$ (pink) becomes irrelevant; ii) Z (yellow) interacts with non-hydrodynamic modes.

From high T to intermediate T : The first step can be seen in the intermediate T regime. In Fig. 10, as T is lowered from Fig. 10(a) to Fig. 10(f), one can see that $Z1$ (pink) is interacting with the non-hydrodynamic mode (E) and goes in the higher frequency regime (i.e., $Z1$ (pink) is moving upward from Fig. 10(a) to Fig. 10(f)). Thus, at intermediate T (e.g., Fig. 10(f)), $Z1$ does not contribute to the low T result.

From intermediate T to low T : Based on the previous paragraph, we have the representative result of intermediate T in Fig. 9(b). Comparing Fig. 9(b) and Fig. 9(c), now

²⁰In order to deliver the main message clearly, we only display the imaginary part of the quasi-normal modes in the paper.

²¹For the energy diffusion case, the collision between the hydrodynamic mode and the non-hydrodynamic mode appears at complex k at low T [51, 66] and real k at high T [47, 80]. On the other hand, for the charge diffusion, the collision occurs at real k for all T as we will show below. Therefore, dynamics from the energy diffusion would be more complicated than the charge diffusion case.

²²At $m/T = 0$, one can obtain the quasi-normal modes at higher temperature ($T \rightarrow \infty$). However, the qualitative structure of the quasi-normal modes does not change, i.e., Fig. 9(a) can be considered as the high enough temperature case.

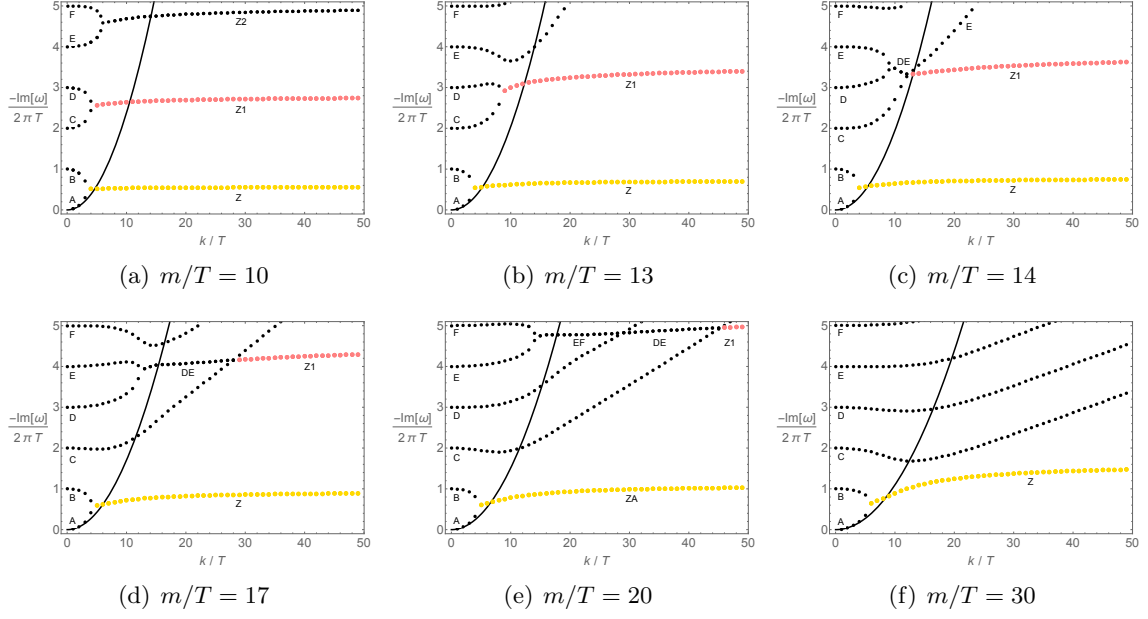


Figure 10. Quasi-normal modes from high T to intermediate T . DE in Fig. 10(c) is made by the collision between D and E . EF in Fig. 10(e) is made by the collision between E and F .

one can see that Z is important for the low T result. For instance, interacting with C (green), Z (yellow) results in two major consequences:

- **Splitting effect:** Z is splitting C into two parts ($C1$, $C2$).
- **Appearance of new line:** while splitting, Z makes a new line CZ (black dots).

Similar behavior also occurs in the interaction between D (blue) and Z (yellow), i.e., D is separated into two parts ($D1$, $D2$) and DZ appears.

The splitting effect is important for the IR modes (A.10) (e.g., for the first non-hydrodynamic mode, one needs not only B , but also $C2$) and the appearance of new line has its significance for the hydrodynamic mode (2.7) (e.g., at lower T , CZ and DZ will be matched with (2.7)). Therefore, Z in high T plays an important role for the low T result.

References

- [1] S. A. Hartnoll, A. Lucas and S. Sachdev, *Holographic quantum matter*, [1612.07324](#).
- [2] J. Zaanen, Y.-W. Sun, Y. Liu and K. Schalm, *Holographic Duality in Condensed Matter Physics*. Cambridge Univ. Press, 2015.
- [3] M. Ammon and J. Erdmenger, *Gauge/gravity duality*. Cambridge Univ. Pr., Cambridge, UK, 2015.
- [4] M. Baggioli, *Applied Holography: A Practical Mini-Course*. SpringerBriefs in Physics. Springer, 2019, [10.1007/978-3-030-35184-7](#).

- [5] J. Erdmenger, B. Herwerth, S. Klug, R. Meyer and K. Schalm, *S-Wave Superconductivity in Anisotropic Holographic Insulators*, *JHEP* **05** (2015) 094, [[1501.07615](#)].
- [6] K.-Y. Kim, K. K. Kim and M. Park, *A Simple Holographic Superconductor with Momentum Relaxation*, *JHEP* **04** (2015) 152, [[1501.00446](#)].
- [7] K. K. Kim, M. Park and K.-Y. Kim, *Ward identity and Homes' law in a holographic superconductor with momentum relaxation*, *JHEP* **10** (2016) 041, [[1604.06205](#)].
- [8] K.-Y. Kim and C. Niu, *Homes' law in Holographic Superconductor with Q-lattices*, *JHEP* **10** (2016) 144, [[1608.04653](#)].
- [9] G. Policastro, D. Son and A. Starinets, *The Shear viscosity of strongly coupled $N=4$ supersymmetric Yang-Mills plasma*, *Phys.Rev.Lett.* **87** (2001) 081601, [[hep-th/0104066](#)].
- [10] J. Zaanen, *Superconductivity: Why the temperature is high*, *Nature* **430** (07, 2004) 512–513.
- [11] S. Sachdev and B. Keimer, *Quantum Criticality*, *Phys. Today* **64N2** (2011) 29, [[1102.4628](#)].
- [12] T. Schäfer and D. Teaney, *Nearly Perfect Fluidity: From Cold Atomic Gases to Hot Quark Gluon Plasmas*, *Rept. Prog. Phys.* **72** (2009) 126001, [[0904.3107](#)].
- [13] S. Cremonini, *The Shear Viscosity to Entropy Ratio: A Status Report*, *Mod. Phys. Lett. B* **25** (2011) 1867–1888, [[1108.0677](#)].
- [14] M. Luzum and P. Romatschke, *Conformal Relativistic Viscous Hydrodynamics: Applications to RHIC results at $s(NN)^{1/2} = 200$ -GeV*, *Phys. Rev. C* **78** (2008) 034915, [[0804.4015](#)].
- [15] J. L. Nagle, I. G. Bearden and W. A. Zajc, *Quark-Gluon Plasma at RHIC and the LHC: Perfect Fluid too Perfect?*, *New J. Phys.* **13** (2011) 075004, [[1102.0680](#)].
- [16] C. Shen, U. Heinz, P. Huovinen and H. Song, *Radial and elliptic flow in Pb+Pb collisions at the Large Hadron Collider from viscous hydrodynamic*, *Phys. Rev. C* **84** (2011) 044903, [[1105.3226](#)].
- [17] L. Alberte, M. Baggioli and O. Pujolas, *Viscosity bound violation in holographic solids and the viscoelastic response*, *JHEP* **07** (2016) 074, [[1601.03384](#)].
- [18] S. A. Hartnoll, D. M. Ramirez and J. E. Santos, *Entropy production, viscosity bounds and bumpy black holes*, *JHEP* **03** (2016) 170, [[1601.02757](#)].
- [19] P. Burikham and N. Poovuttikul, *Shear viscosity in holography and effective theory of transport without translational symmetry*, *Phys. Rev. D* **94** (2016) 106001, [[1601.04624](#)].
- [20] A. Rebhan and D. Steineder, *Violation of the Holographic Viscosity Bound in a Strongly Coupled Anisotropic Plasma*, *Phys. Rev. Lett.* **108** (2012) 021601, [[1110.6825](#)].
- [21] S. Jain, R. Samanta and S. P. Trivedi, *The Shear Viscosity in Anisotropic Phases*, *JHEP* **10** (2015) 028, [[1506.01899](#)].
- [22] D. Giataganas, *Observables in Strongly Coupled Anisotropic Theories*, *PoS Corfu2012* (2013) 122, [[1306.1404](#)].
- [23] V. Jahnke, A. S. Misobuchi and D. Trancanelli, *Holographic renormalization and anisotropic black branes in higher curvature gravity*, *JHEP* **01** (2015) 122, [[1411.5964](#)].
- [24] G. A. Inkof, J. M. C. Küppers, J. M. Link, B. Goutéraux and J. Schmalian, *Quantum critical scaling and holographic bound for transport coefficients near Lifshitz points*, *JHEP* **11** (2020) 088, [[1907.05744](#)].
- [25] M. Brigante, H. Liu, R. C. Myers, S. Shenker and S. Yaida, *Viscosity Bound Violation in*

- Higher Derivative Gravity*, *Phys. Rev.* **D77** (2008) 126006, [[0712.0805](#)].
- [26] M. Brigante, H. Liu, R. C. Myers, S. Shenker and S. Yaida, *The Viscosity Bound and Causality Violation*, *Phys. Rev. Lett.* **100** (2008) 191601, [[0802.3318](#)].
 - [27] M. Baggioli and W.-J. Li, *Universal Bounds on Transport in Holographic Systems with Broken Translations*, *SciPost Phys.* **9** (2020) 007, [[2005.06482](#)].
 - [28] M. Baggioli, K.-Y. Kim, L. Li and W.-J. Li, *Holographic Axion Model: a simple gravitational tool for quantum matter*, [2101.01892](#).
 - [29] M. Blake, *Universal Charge Diffusion and the Butterfly Effect in Holographic Theories*, *Phys. Rev. Lett.* **117** (2016) 091601, [[1603.08510](#)].
 - [30] M. Blake, *Universal Diffusion in Incoherent Black Holes*, *Phys. Rev.* **D94** (2016) 086014, [[1604.01754](#)].
 - [31] A. Lucas, *Operator size at finite temperature and Planckian bounds on quantum dynamics*, *Phys. Rev. Lett.* **122** (2019) 216601, [[1809.07769](#)].
 - [32] R. A. Davison, S. A. Gentle and B. Goutéraux, *Slow relaxation and diffusion in holographic quantum critical phases*, *Phys. Rev. Lett.* **123** (2019) 141601, [[1808.05659](#)].
 - [33] Y. Gu, A. Lucas and X.-L. Qi, *Spread of entanglement in a Sachdev-Ye-Kitaev chain*, *JHEP* **09** (2017) 120, [[1708.00871](#)].
 - [34] Y. Ling and Z.-Y. Xian, *Holographic Butterfly Effect and Diffusion in Quantum Critical Region*, *JHEP* **09** (2017) 003, [[1707.02843](#)].
 - [35] Y. Gu, A. Lucas and X.-L. Qi, *Energy diffusion and the butterfly effect in inhomogeneous Sachdev-Ye-Kitaev chains*, [1702.08462](#).
 - [36] M. Blake and A. Donos, *Diffusion and Chaos from near AdS_2 horizons*, *JHEP* **02** (2017) 013, [[1611.09380](#)].
 - [37] M. Blake, R. A. Davison and S. Sachdev, *Thermal diffusivity and chaos in metals without quasiparticles*, [1705.07896](#).
 - [38] S.-F. Wu, B. Wang, X.-H. Ge and Y. Tian, *Collective diffusion and quantum chaos in holography*, *Phys. Rev. D* **97** (2018) 106018, [[1702.08803](#)].
 - [39] W. Li, S. Lin and J. Mei, *Thermal diffusion and quantum chaos in neutral magnetized plasma*, *Phys. Rev. D* **100** (2019) 046012, [[1905.07684](#)].
 - [40] X.-H. Ge, S.-J. Sin, Y. Tian, S.-F. Wu and S.-Y. Wu, *Charged BTZ-like black hole solutions and the diffusivity-butterfly velocity relation*, *JHEP* **01** (2018) 068, [[1712.00705](#)].
 - [41] W.-J. Li, P. Liu and J.-P. Wu, *Weyl corrections to diffusion and chaos in holography*, *JHEP* **04** (2018) 115, [[1710.07896](#)].
 - [42] H.-S. Jeong, Y. Ahn, D. Ahn, C. Niu, W.-J. Li and K.-Y. Kim, *Thermal diffusivity and butterfly velocity in anisotropic Q -Lattice models*, *JHEP* **01** (2018) 140, [[1708.08822](#)].
 - [43] M. Baggioli and W.-J. Li, *Diffusivities bounds and chaos in holographic Horndeski theories*, *JHEP* **07** (2017) 055, [[1705.01766](#)].
 - [44] K.-Y. Kim and C. Niu, *Diffusion and Butterfly Velocity at Finite Density*, *JHEP* **06** (2017) 030, [[1704.00947](#)].
 - [45] A. Amoretti, A. Braggio, N. Magnoli and D. Musso, *Bounds on charge and heat diffusivities in momentum dissipating holography*, *JHEP* **07** (2015) 102, [[1411.6631](#)].

- [46] M. Blake, R. A. Davison, S. Grozdanov and H. Liu, *Many-body chaos and energy dynamics in holography*, *JHEP* **10** (2018) 035, [[1809.01169](#)].
- [47] H.-S. Jeong, K.-Y. Kim and Y.-W. Sun, *Bound of diffusion constants from pole-skipping points: spontaneous symmetry breaking and magnetic field*, [2104.13084](#).
- [48] M. Baggioli, B. Goutéraux, E. Kiritsis and W.-J. Li, *Higher derivative corrections to incoherent metallic transport in holography*, [1612.05500](#).
- [49] A. Lucas and J. Steinberg, *Charge diffusion and the butterfly effect in striped holographic matter*, *JHEP* **10** (2016) 143, [[1608.03286](#)].
- [50] R. A. Davison, W. Fu, A. Georges, Y. Gu, K. Jensen and S. Sachdev, *Thermoelectric transport in disordered metals without quasiparticles: the SYK models and holography*, [1612.00849](#).
- [51] D. Arean, R. A. Davison, B. Goutéraux and K. Suzuki, *Hydrodynamic Diffusion and Its Breakdown near AdS₂ Quantum Critical Points*, *Phys. Rev. X* **11** (2021) 031024, [[2011.12301](#)].
- [52] T. Hartman, S. A. Hartnoll and R. Mahajan, *Upper Bound on Diffusivity*, *Phys. Rev. Lett.* **119** (2017) 141601, [[1706.00019](#)].
- [53] A. Lucas, *Constraints on hydrodynamics from many-body quantum chaos*, [1710.01005](#).
- [54] B. Withers, *Short-lived modes from hydrodynamic dispersion relations*, *JHEP* **06** (2018) 059, [[1803.08058](#)].
- [55] S. Grozdanov, P. K. Kovtun, A. O. Starinets and P. Tadić, *Convergence of the Gradient Expansion in Hydrodynamics*, *Phys. Rev. Lett.* **122** (2019) 251601, [[1904.01018](#)].
- [56] S. Grozdanov, P. K. Kovtun, A. O. Starinets and P. Tadić, *The complex life of hydrodynamic modes*, *JHEP* **11** (2019) 097, [[1904.12862](#)].
- [57] M. P. Heller, A. Serantes, M. Spaliński, V. Svensson and B. Withers, *Convergence of hydrodynamic modes: insights from kinetic theory and holography*, [2012.15393](#).
- [58] M. P. Heller, A. Serantes, M. Spaliński, V. Svensson and B. Withers, *The hydrodynamic gradient expansion in linear response theory*, [2007.05524](#).
- [59] M. P. Heller, R. A. Janik and P. Witaszczyk, *Hydrodynamic Gradient Expansion in Gauge Theory Plasmas*, *Phys. Rev. Lett.* **110** (2013) 211602, [[1302.0697](#)].
- [60] N. Abbasi and S. Tahery, *Complexified quasinormal modes and the pole-skipping in a holographic system at finite chemical potential*, *JHEP* **10** (2020) 076, [[2007.10024](#)].
- [61] A. Jansen and C. Pantelidou, *Quasinormal modes in charged fluids at complex momentum*, *JHEP* **10** (2020) 121, [[2007.14418](#)].
- [62] S. Grozdanov, *Bounds on transport from univalence and pole-skipping*, *Phys. Rev. Lett.* **126** (2021) 051601, [[2008.00888](#)].
- [63] C. Choi, M. Mezei and G. Sárosi, *Pole skipping away from maximal chaos*, [2010.08558](#).
- [64] S. Grozdanov, A. Starinets and P. Tadić, *Hydrodynamic dispersion relations at finite coupling*, [2104.11035](#).
- [65] N. Wu, M. Baggioli and W.-J. Li, *On the universality of AdS₂ diffusion bounds and the breakdown of linearized hydrodynamics*, *JHEP* **05** (2021) 014, [[2102.05810](#)].
- [66] H.-S. Jeong, K.-Y. Kim and Y.-W. Sun, *The breakdown of magneto-hydrodynamics near*

AdS₂ fixed point and energy diffusion bound, [2105.03882](#).

- [67] T. Andrade and B. Withers, *A simple holographic model of momentum relaxation*, *JHEP* **1405** (2014) 101, [[1311.5157](#)].
- [68] S. A. Hartnoll, *Theory of universal incoherent metallic transport*, *Nature Phys.* **11** (2015) 54, [[1405.3651](#)].
- [69] P. K. Kovtun and A. O. Starinets, *Quasinormal modes and holography*, *Phys. Rev.* **D72** (2005) 086009, [[hep-th/0506184](#)].
- [70] M. Baggioli, *How small hydrodynamics can go*, *Phys. Rev. D* **103** (2021) 086001, [[2010.05916](#)].
- [71] M. Baggioli, V. V. Brazhkin, K. Trachenko and M. Vasin, *Gapped momentum states*, *Phys. Rept.* **865** (2020) 1–44, [[1904.01419](#)].
- [72] M. Blake, R. A. Davison and D. Vegh, *Horizon constraints on holographic Green’s functions*, [1904.12883](#).
- [73] Y. Ahn, V. Jahnke, H.-S. Jeong, C.-W. Ji, K.-Y. Kim and M. Nishida, *General and systematic understanding of pole-skipping points*, to appear (2021) .
- [74] O. Bohigas, *Characterization of chaotic quantum spectra and universality of level fluctuation laws*, *Physical Review Letters* **52** (1984) 1–4.
- [75] B. M. Victor, T. M and Z. J. Michael, *Level clustering in the regular spectrum*, *Proc. R. Soc. Lond. A* **356** (Set, 1977) .
- [76] M. Berry, *Quantizing a classically ergodic system: Sinai’s billiard and the kkr method*, *Annals of Physics* **131** (1981) 163–216.
- [77] Y. Liu and X.-M. Wu, *Breakdown of hydrodynamics from holographic pole collision*, [2111.07770](#).
- [78] T. Faulkner, H. Liu, J. McGreevy and D. Vegh, *Emergent quantum criticality, Fermi surfaces, and AdS(2)*, *Phys.Rev.* **D83** (2011) 125002, [[0907.2694](#)].
- [79] S. A. Hartnoll and D. M. Hofman, *Locally Critical Resistivities from Umklapp Scattering*, *Phys.Rev.Lett.* **108** (2012) 241601, [[1201.3917](#)].
- [80] R. A. Davison and B. Goutéraux, *Momentum dissipation and effective theories of coherent and incoherent transport*, [1411.1062](#).